Journal of Polymer Research (2023) 30:116
https://doi.org/10.1007/s10965-023-03497-w

ORIGINAL PAPER

A one-pot water mediated process for developing conductive composites with segregated network of poly(3,4-ethylenedioxythiophene) on spherical poly(methyl methacrylate) particles

P A Saeed[1,2] · K Juraij[1] · P M Saharuba[1] · A Sujith[1]

Received: 28 November 2022 / Accepted: 15 February 2023 / Published online: 24 February 2023

Abstract
Conductive polymer composites (CPCs) with segregated networks are highly desirable for lowering the percolation threshold as well as the synergetic upgrading of electrical and thermal properties. Here we disclose a one-pot water mediated process for developing conductive composite of poly(methyl methacrylate) (PMMA) with dense poly(3,4-ethylenedioxythiophene) (PEDOT) surface as segregated conductive channel. The key idea is the judicious handling of surface charges of PMMA latex and 3,4-ethylenedioxythiophene (EDOT) emulsion which are prepared using surfactant free emulsion polymerization and acoustic emulsification, respectively. The obtained composite shows refinement in material properties as compared to the composites prepared using conventional methods. The composite provides about ~10^5 and ~10^7 fold increase in electrical conductivity as compared to the composites prepared by the direct addition of EDOT to the PMMA latex and physical blending of PMMA with PEDOT bulk particles, respectively. Additionally it shows ~ 10^{11} fold increase in electrical conductivity compared with the PMMA matrix. This method opens up a new path in sustainable materials research for the synthesis of conductive polymer composites.

Keywords PMMA · PEDOT · Segregated structure

Introduction

The development of electrically conductive polymer composites (CPCs) with segregated networks has been a fast progressing field of materials science [1–4]. It exploits the synergetic effect of participating materials in a great extent. In particular, CPCs composed of conducting and insulating polymers have important applications in many areas such as antistatic materials [5], electromagnetic interference shielding [3, 6], electronic devices [7, 8], and sensors [9, 10]. Compared to the single polymers, CPCs are highly promising materials with advantages of tunable electrical and mechanical properties.

✉ A Sujith
sujith@nitc.ac.in

[1] Materials Research Laboratory, Department of Chemistry, National Institute of Technology Calicut, 673601 Calicut, Kerala, India

[2] Department of Chemistry, Government Engineering College Wayanad, 670644 Thalappuzha, Kerala, India

However, the conventional methods for the synthesis of such materials are facing some challenging issues. One of the major issues is the need of harmful solvents and surfactants which makes significant environmental issues and poor economic affordability [7, 11, 12]. Secondly, the need of high percolation threshold, which critically limits the mechanical properties [8, 13, 14]. Percolation threshold refers a critical value of conducting polymer content where the electrical conductivity of the material dramatically increases by the formation of conductive channels. Commonly adopted methods including melt mixing, solution processing, and in situ polymerization have been criticized by such critical issues partially or completely [2, 7, 15].

In this scenario, a one-pot water mediated method for the synthesis of conductive composites composed of a conducting polymer and an insulating polymer with segregated structure becomes significant. The use of water as reaction medium provides, low cost and safer benefits for polymerization process. Among various conducting polymers (CPs), poly (3,4-ethylenedioxythiophene) (PEDOT) is widely studied with the merits of remarkable conductivity and environmental stability [16–20]. Interestingly, the acoustic

emulsification method, produces the emulsion of EDOT (3,4-ethylenedioxythiophene) monomer without the use of surfactants [21, 22]. The ultrasonic irradiation generates the mechanical force at the liquid/liquid phase boundaries which finally results the emulsion droplets with a milky white nature [23–26]. Fogler et al. suggested that the acoustic emulsions can be stabilized by the preferentially adsorbed OH^- ions from the aqueous medium [27–29].

On the other hand, poly(methyl methacrylate) (PMMA) is an important insulating matrix polymer with superior mechanical strength and optical clarity [30, 31]. It has widespread attention in interface science since it can form stable latex particles [32, 33]. Moreover its ester groups can help for the integration with CPs by non-bonded interactions which are crucial in the designing of CPCs [7, 34]. Many processes for preparing such CPCs were developed in the past few years. In particular, latex based colloidal blending has attracted remarkable attention since it supports for the formation of segregated conductive channel via effective filling of CPs into the interstitial spaces of matrix polymer [2, 32]. However its practical applications are limited in aspect of non-greener, increase of cost, difficulty of purification, and inferior conductive nature. Contrary, PMMA latex particles with cationic surface can be prepared using surfactant-free emulsion polymerization in water medium [32, 33].

In this study, we discuss the synthesis of conductive polymer composites of PMMA microspheres with surface enriched PEDOT via a one-pot water mediated method. For this goal, we focus to utilize the advantage of surface charges of PMMA latex and EDOT emulsion. The composite is prepared by three successive steps, executed in a one-pot reaction container equipped with deionized water at 75 °C under N_2 atmosphere. The cationic PMMA particles invite the anionic EDOT monomers towards its surface and followed by the in situ oxidative polymerization, resulting densely wrapped PEDOT on PMMA microsphere. The obtained polymer composite exhibits segregated conductive networks in the insulating matrix, which is beneficial to the electrical and thermal properties. Due to the absence of harmful solvents and surfactants, process becomes simpler and greener alternative to the conventional methods.

Experimental section

Materials

The following chemicals were used without further purification. Methyl methacrylate (MMA, reagent grade, 99%, Alfa Aeser), 3,4-ethylenedioxythiophene (EDOT, reagent grade, 97%, Alfa Aeser), 2,2′-Azobis(2-methylpropionamidine) dihydrochloride (AIBA, reagent grade, 97% Sigma Aldrich), and Iron(III) p-toluenesulfonate hexahydrate (Ferric tosylate, FeTS, technical grade, Sigma Aldrich), poly(methyl methacrylate) (PMMA, Mw ~ 120,000, Sigma Aldrich).

Preparation of EDOT emulsion

The acoustic emulsification method has been followed to obtain the anionic EDOT emulsion [25]. Typically, 100 µL of EDOT monomer was ultrasonically emulsified in 10 mL of DI water using a probe sonicator (5 mm diameter, titanium alloy) connected with a 20 kHz oscillator for 2 min. To neutralize the excess heat produced, a cooling bath was used.

Preparation of composites with surface enriched PEDOT on PMMA microspheres

The composite was successfully synthesized by a benign one-pot approach. Initially, a one-pot vessel (three neck RB flask) was equipped with 87.5 mL of DI water at 75 °C, 350 rpm, and under nitrogen atmosphere. This experimental setup was kept as constant for whole process. In the first step, the addition of MMA (10 g) was carried out carefully and subsequently added the aqueous solution (2.5 mL) of AIBA (0.015 g) and kept for 5 h. During the second step, acoustically emulsified EDOT was gradually added and kept for 30 min. In the final step, aqueous FeTS was slowly added and kept for 24 h. The EDOT/FeTS mole ratio was taken as 1:2. The obtained polymer composite with dark blue color was washed with DI water. Finally, a methanol washing was also conducted and dried at 70 °C.

Preparation of composites by the direct addition of EDOT to the PMMA latex

The composite was synthesized by following the above procedure without using acoustic emulsification method. Instead, 100 µL of EDOT monomer was directly added. In short, a one pot vessel (three neck RB flask) was equipped with 87.5 mL of DI water at 75 °C, 350 rpm, and under nitrogen atmosphere. Then MMA (10 g) was added carefully and subsequently added the aqueous solution (2.5 mL) of AIBA (0.015 g) and kept for 5 h. Then, 100 µL of EDOT monomer was directly added and kept for 30 min. Finally, aqueous FeTS was slowly added and kept for 24 h. The EDOT/FeTS mole ratio was taken as 1:2. The obtained polymer composite was washed and dried at 70 °C.

Preparation of PEDOT bulk powder

About 100 µL of EDOT monomer was added to 97.5 mL of DI water taken in a RB flask and then the temperature was gradually

increased to 75 °C. Then aqueous FeTS was slowly added and kept for 24 h. the EDOT/FeTS mole ratio was taken as 1:2. The obtained polymer composite was washed and dried at 70 °C.

Preparation of composites by the physical blending of PMMA and PEDOT bulk particles

About 0.9 g of PMMA and 0.1 g of PEDOT powders were mixed and crushed using a mortar and pestle. Then the mixture was compression molded in a hydraulic hot press (Mini Metal) at 40 bar with a temperature of 200 °C for 10 min.

Characterization

To study the morphologies of PMMA and composite microspheres, field emission scanning electron microscopy (FE-SEM, Hitachi 6600) and high-resolution transmission electron microscopy (HRTEM, JOEL JEM-2100) were used. The compositional studies were conducted using energy dispersive X-ray analysis (EDX, Jeol 6390LA/Oxford XMX N) and X-ray photoelectron spectroscopy (XPS, PHI 5000 ESCA). X-ray diffraction analysis (XRD) and Fourier Transform Infrared Spectroscopy (FT-IR) were conducted on Rigaku MiniFlex 600 diffractometer and Nicolet 5700, respectively. Thermogravimetric analysis (TGA) and differential scanning calorimetry (DSC) were performed on TA Q50 and TA Q20 (heating rate of 10 °C/min, N_2 atmosphere), respectively. The surface charge was analyzed using zetasizer (Nano ZS, Malvern). For electrical resistance measurements four-point probe method was used on Keithley 2450. The powder samples were converted to pellets. The measured thickness using digital screw gauge and the diameter of the pellets were 0.3 to 0.5 mm and 1 cm, respectively. The distance between the nearby probes is 0.15 cm. The constant for calculation depends on diameter of the pellet and the distance between the nearby probes. For our measurements, it is 3.7. The following equations were used to calculate the electrical conductivity,

$$\text{Resistivity}(\rho) = \text{Resistance} \times \text{thickness} \times \text{constant}$$

$$\text{Conductivity}(\sigma) = \frac{1}{\rho}$$

Results and discussion

Formation of surface enriched PEDOT on PMMA microsphere

Figure 1 illustrates the detailed procedure for the synthesis of PMMA microcomposite with dense PEDOT surface. For the entire process, a one-pot reaction flask was equipped with deionized water at 75 °C temperature under

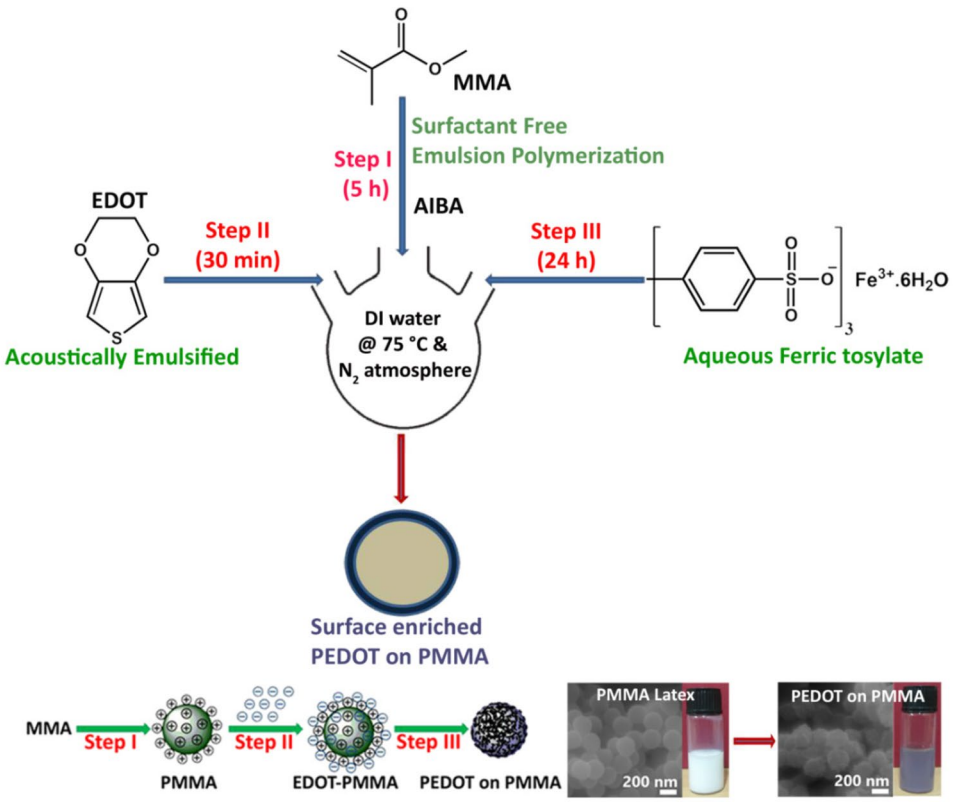

Fig. 1 Schematic procedure for preparing microcomposite of PMMA with dense PEDOT surface

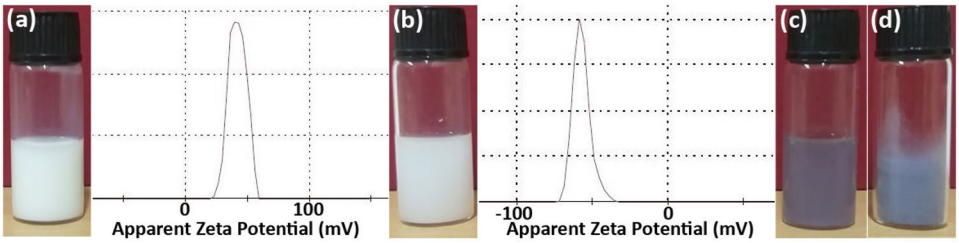

Fig. 2 Photographs and Zeta potential distributions of **a** PMMA latex and **b** EDOT emulsion. Photographs of **c** aqueous dispersion and **d** powder form of polymer composite

N_2 atmosphere. Then three successive steps were involved. In the first step, PMMA microsphere latex was prepared using surfactant free emulsion polymerization which could create surface positive charge due to the decomposition of initiator [35]. The zeta potential of the PMMA latex was measured as +41.7 mV. The photograph of PMMA latex and the zeta potential distribution is shown in Fig. 2a. The measured molecular weight of PMMA particle is 36714 g/mol. Secondly, the slow addition of anionic EDOT which was prepared by acoustic emulsification generates EDOT accumulated PMMA microsphere via electrostatic interaction.

Figure 2b shows the photograph of acoustic EDOT emulsion and its zeta potential distribution which was measured as −57.3 mV, respectively. Zeta potential distributions of other EDOT samples are exhibited in Fig. S1. In the final step, the in-situ oxidative polymerization of accumulated EDOT was carried out using aqueous ferric tosylate, resulting PMMA microcomposite with surface enriched PEDOT. The aqueous dispersion (2 mg/mL) and powder form of the polymer composite are shown in Fig. 2c, d.

During the final step, cationic PMMA microspheres play a significant role of compactable template for EDOT polymerization, leading to the formation of PEDOT wrapped PMMA with dense conductive network. The whole reaction processes were carried out in water media, making it green and simple. Also, the other two conventional composites were synthesized separately. Firstly, prepared by the direct addition of EDOT to the PMMA latex and secondly, by the physical blending of PMMA and PEDOT bulk particles (see Experimental section).

Morphology of the microcomposite

TEM analysis was carried out to exhibits the surface enriched PEDOT on PMMA microsphere and thereby generating the segregated conductive network (Fig. 3). Figure 3a, b show PMMA particles are spherical, fine surface, and the size range of 195 nm. The morphologies of microcomposites with increasing the wt% of PEDOT contents are presented in Fig. 3c-e. Composites show totally a different morphology compared with the smooth PMMA microsphere. An irregular surface with enriched PEDOT layer is formed. The average thickness of PEDOT layer is about 15 nm. It indicates the existence of segregated structure which is crucial for the generation of conductive channel.

Even at 4.7 wt% of PEDOT content (Fig. 3c), the dense interconnected PEDOT network is clearly visible. In addition, it validates a core-shell morphology in which the spherical PMMA core is wrapped with a shell of in-situ polymerized PEDOT particles. Obviously, this morphology substantiates the refinement in the electrical and thermal properties of composite materials which will be discussed in later section.

In order to further observe the network, SEM analysis was also employed. We can distinctly see the uneven surface of microcomposite (Fig. 4b-f) on the spherical PMMA particles (Fig. 4a). Truly, this irregular structure in the surface validates the overlaying of dense PEDOT particles as segregated network. In addition, the conducting particles are heavily distributed between the interstitial spaces of PMMA microspheres. During the oxidative polymerization, the formation and the spontaneous assembling of EDOT

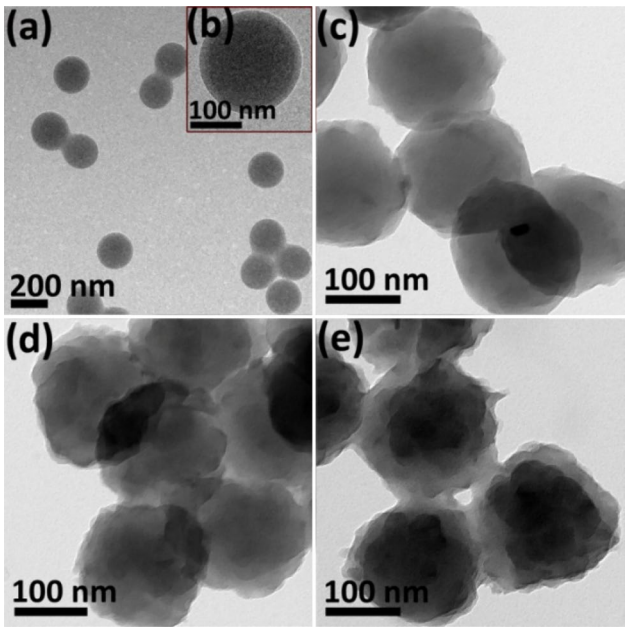

Fig. 3 TEM images of PMMA and composites with varying PEDOT contents: **a** and **b** PMMA, **c** 4.70 wt%, **d** 6.23 wt%, and **e** 7.31 wt% respectively

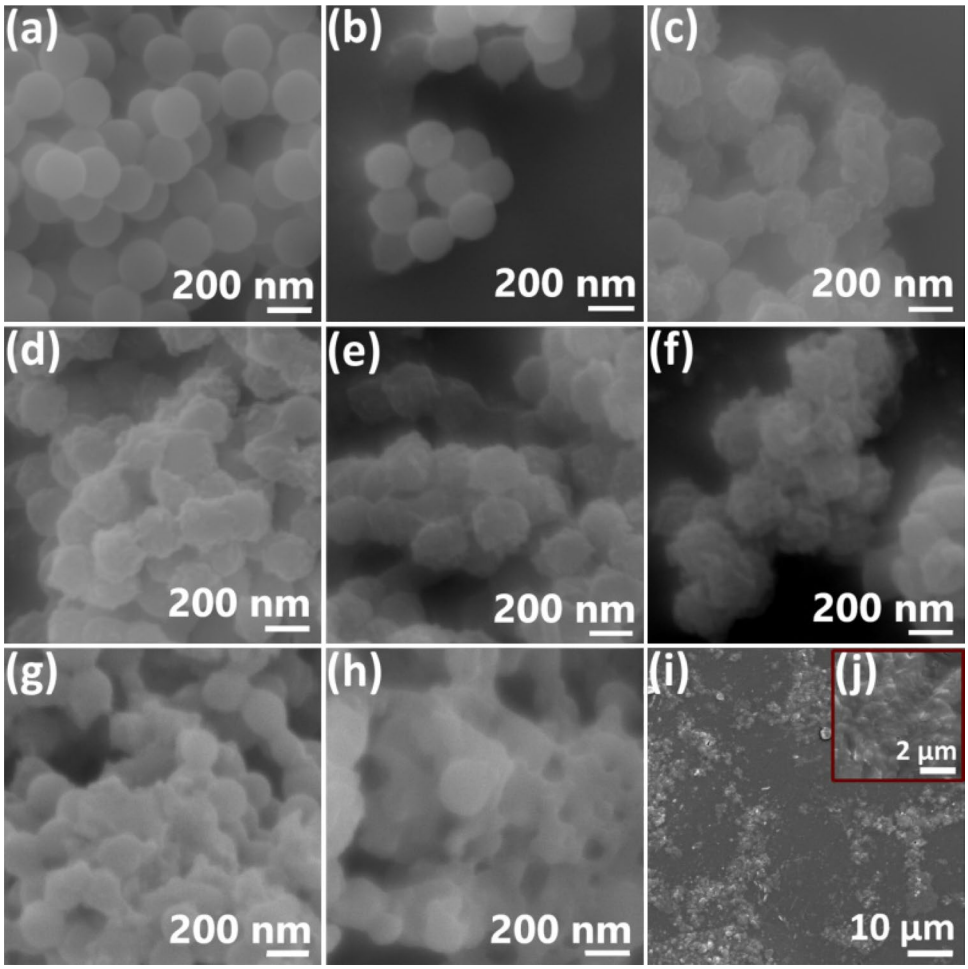

Fig. 4 SEM images: **a** PMMA particles, composites with varying PEDOT loading **b** 2.76 wt%, **c** 4.70 wt%, **d** 6.23 wt%, **e** 7.31 wt%, **f** 13.54 wt%, composite formed from direct addition of EDOT **g** 9.6 wt%, **h** 15.9 wt%, composite formed by physical blending of PEDOT and PMMA **i** 10 wt%, and **j** magnified image, respectively

oligomers were occurred and thus resulting composite with surface enriched PEDOT on PMMA microsphere. However, at higher PEDOT content (Fig. 4f), partially agglomerated PEDOT layer occurs which is not beneficial for improving electrical and thermal properties.

Interestingly, the other two composites prepared by the direct addition of EDOT to the PMMA latex (Fig. 4g, h) and the physical blending of PMMA and PEDOT (Fig. 4i, j) respectively, exhibited non-uniform distribution of PEDOT. Figure 4g, h represents the composite with 9.6 wt% and 15.9 wt% PEDOT loading, respectively. It shows a non-uniform PEDOT surface with agglomerated morphologies. Similarly, the composite formed with 10 wt% of PEDOT powder by physical blending (Fig. 4i, j) shows uneven distribution of PEDOT particles throughout the PMMA matrix. In both cases, the absence of segregated networks limits the overall conductivity of the composite.

Structural characteristics

Further, the formation of composite was confirmed by FT-IR spectra, XPS spectra and XRD analysis.

The FT-IR spectra (Fig. 5a) of pure PEDOT exhibited main peaks at 1522 cm^{-1}, 1353 cm^{-1}, 1094 cm^{-1}, and 979 cm^{-1} are assigned to the stretching vibrations of C = C, C-C, C-O, and C-S bonds, respectively [14, 36]. For PMMA, the exhibited dominant peaks at 1731 cm^{-1} and 1150 cm^{-1} are assigned to the presence of C = O and C-O stretching vibrations, respectively [7]. Compared to the polymers alone, composite shows peak mainly at 1722 cm^{-1} and 1518 cm^{-1}. It is assigned to the C = O of PMMA and C = C of thiophene ring, respectively. It indicates, PEDOT has been integrated to the composite during the process. Upon integration, the peak position was shifted suggesting the electrostatic and interfacial interactions between the polymers.XPS analysis was used to quantify the chemical composition at the surface and also to verify the successful integration of PEDOT on PMMA microspheres (Fig. 5b). A detailed discussion on quantification has been included in the next section. In the survey spectrum of composite, the four peaks appearing approximately at 532.5 eV, 284.6 eV, 228.6 eV, and 163.5 eV can be attributed to O 1s, C 1s, S 2s, and S 2p, respectively [14, 37, 38]. Apart from C 1s and O 1s peaks, signal due to

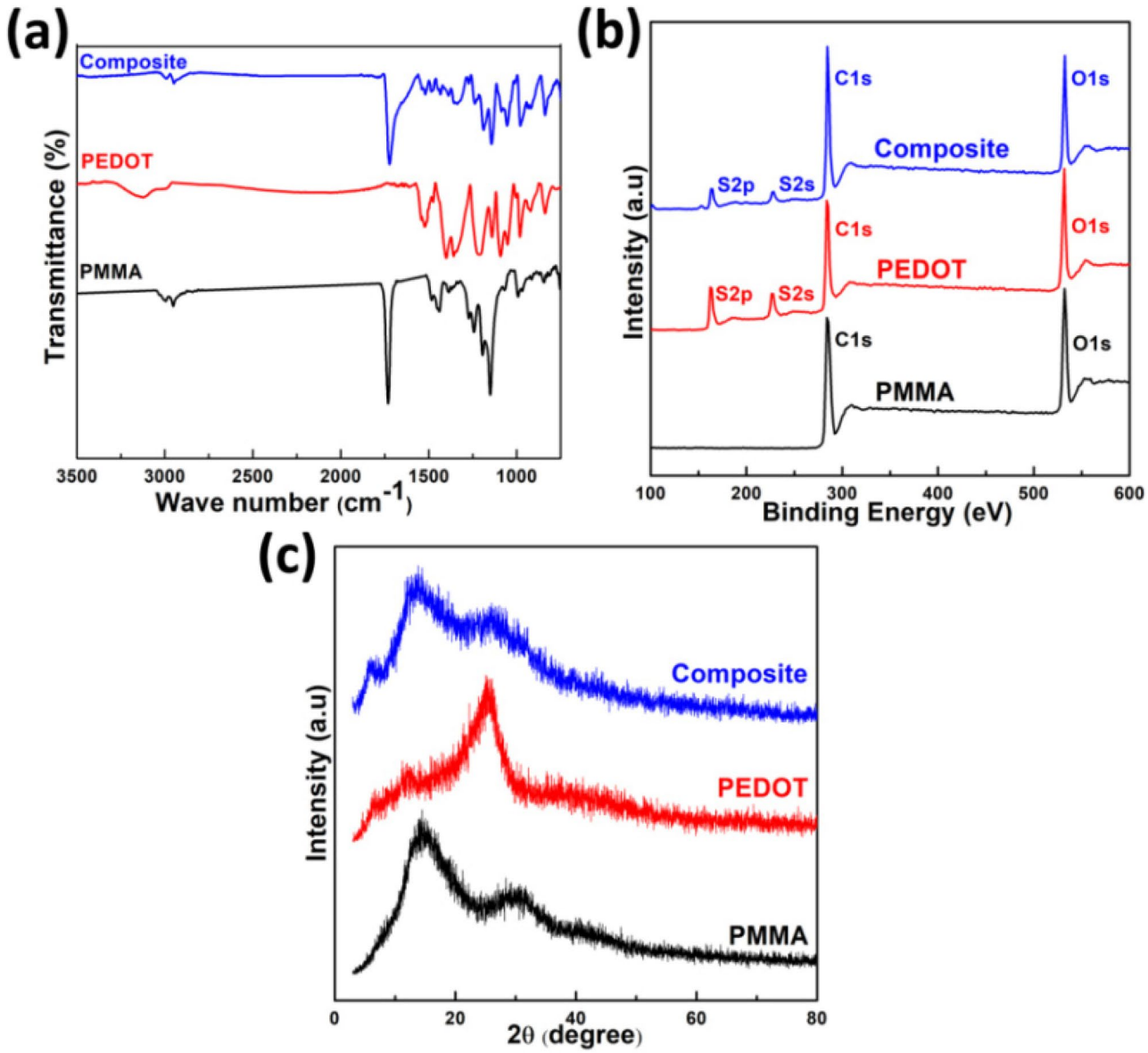

Fig. 5 **a** FTIR spectra, **b** XPS survey spectra, and **c** XRD spectra of composite

sulfur was also present. This S 2s and S 2p signals validate the existence of PEDOT at the surface. Additionally, the relative intensity of signals due to the sulfur content in the composite is lower than PEDOT powder.

The presence of the PEDOT on PMMA is further verified by XRD analysis (Fig. 5c). For PEDOT, the observed peaks at $2\theta = 6.8°$, 11.9°, and 25.4° can be assigned to (1 0 0), (2 0 0), and (0 2 0) reflections, respectively [39]. Differently, PMMA has two broad peaks at $2\theta = 14.5°$ and 30.1°, indicating its amorphous nature [40]. The composite exhibited the peaks at scattering angle of $2\theta = 6.3°$, 13.5°, and 25.7°. It confirms that PEDOT has been incorporated to the PMMA matrix.

Compositional characteristics

To quantify the compositions and the surface deposition of PEDOT in the composite, XPS (Fig. 6) and EDX (Fig. S2) analyses were utilized. The summarized results are given in Table 1. As seen in the survey spectra (Fig. 6a) of composites, the S 2p signal originating from the collective contributions of PEDOT content and the tosylate dopant, are clearly visible. As the PEDOT content is increased, the intensity of S 2p signal also increases. The PEDOT content in the composites was quantified and it varies from 2.76 wt% to 13.54 wt% (Table 1).

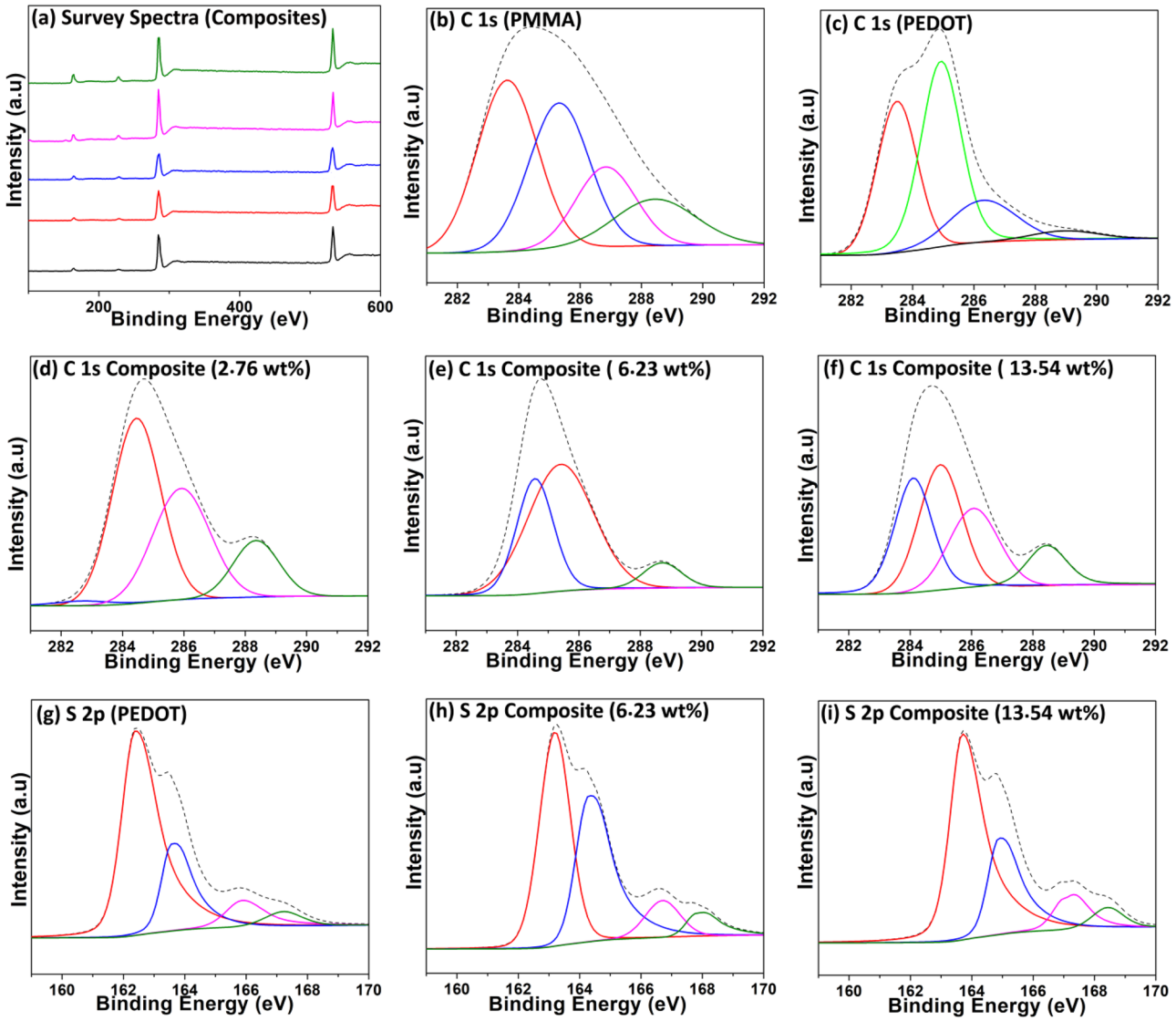

Fig. 6 XPS spectra: **a** survey spectra of composite, C 1s spectra of **b** PMMA, **c** PEDOT, **d-f** composites of 2.76 wt%, 6.23 wt% and 13.54 wt%, respectively. S 2p spectra of **g** PEDOT and **h**, **i** composites of 6.23 wt% and 13.54 wt%, respectively

The deconvoluted C 1s spectra of polymers alone and composites with varying PEDOT contents are shown in Fig. 6b-f. For PMMA (Fig. 6b), the main peaks are assigned to C-C/C-H (283.61 eV), C-C-O (285.31 eV), C-O (286.81 eV), and O-C=O (288.39 eV) [41, 42]. For PEDOT (Fig. 6c), the dominant peaks are attributed to C-C/C-H (283.50 eV), C-S (284.93 eV), and a weak peak for C-O (286.30 eV) [43, 44].

Table 1 Doping Level of Tosylate, Surface Coverage and the Relative Proportions of PEDOT in the Composites

Composite	S (at%) by XPS	% of tosylate dopant	Doping level (%)	PEDOT coverage at the surface (at%)	S (wt%) by EDX	PEDOT (wt%)
Sample I	2.07	16.7	20.04	15.60	0.62	2.76
Sample II	3.66	14.9	17.51	28.13	1.05	4.70
Sample III	4.09	15	17.64	31.39	1.40	6.23
Sample IV	4.81	16	19.04	36.38	1.64	7.31
Sample V	5.84	15	17.64	44.77	3.04	13.54

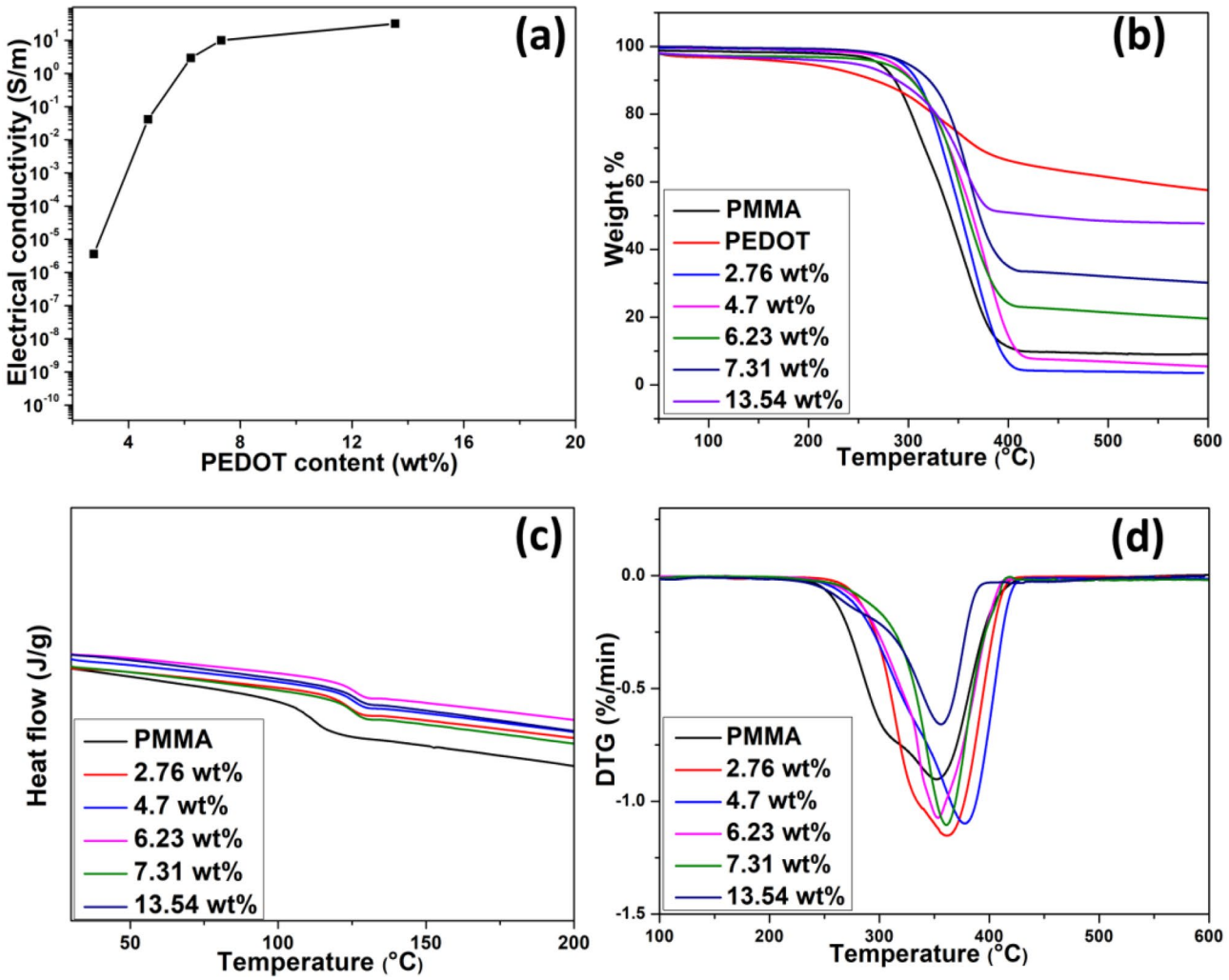

Fig. 7 **a** Electrical conductivity of composites versus PEDOT contents, **b** TGA, **c** DSC and **d** DTG curves

In addition, a weak peak is assigned to π→π* shake up signal of heteroaromatic thiophene ring (289.01 eV). However, for the composites (Fig. 6d-f), some signals are overlapped as compared to the obtained reference spectra of PMMA and PEDOT particles. Moreover, due to the presence of densely wrapped PEDOT, highly loaded composites resemble the peaks of the PEDOT particles.

To calculate the deposition of PEDOT at the surface and the doping level of tosylate anion, S 2p spectra for PEDOT (Fig. 6g) and composites (Fig. 6h,i) was studied. The observed main peaks for PEDOT are attributed to neutral S (162-163.11 eV) and cationic S+ (163.30-165.28 eV) [39, 44, 45]. The additional peaks are assigned to tosylate dopant (166.01-168.95 eV). The doping levels were calculated by comparing the peak areas of tosylate dopant and PEDOT backbone. The relative proportion of tosylate dopant was roughly 18.8 ± 1.2 (Table 1), consistent with previous studies [39].

Further, energy dispersive X-ray analysis (Fig. S2) is used to determine the PEDOT content in the composite. Also the results are summarized in Table 1. As expected, PEDOT content in the composite increases, the intensity of signal due to sulfur also increases. From the calculations of elemental composition and the percentage of tosylate dopant using EDX and XPS analyses respectively, the PEDOT content in the five samples were quantified as 2.76 wt%, 4.70 wt%, 6.23 wt%, 7.31 wt% and 13.54 wt%.

The quantified results of composites have been listed in Table 1 including the surface coverage and the percentage of loading of PEDOT. By taking the atomic ratio (S 2p signal) of composites to the PEDOT alone, the relative percentage of PEDOT at the surface of the composites was estimated. Similarly, the PEDOT content in the composite was determined by comparing the weight ratio of sulfur in the composite to the PEDOT alone, as analyzed from the EDX analysis. Precisely, in such calculations, the sulfur

Table 2 Comparison of Processing Method and Electrical Conductivity of Our One-pot Water Mediated Composite with Several CP Based CPCs

Composite	Integration of CP	Filler content (wt%)	Conductivity (S/m)	Percolation threshold	Remarks
PMMA/PPY [7]	EP[a]	20	50	12.5 wt%	High percolation threshold, use of surfactants
PMMA/PEDOT [8]	SSP[b]	50	1.8	N/A	High filler content, use of organic solvents
PS/PEDOT [8]	SSP[b]	75	275	N/A	High filler content, use of organic solvents
PS/PEDOT [46]	OP[c]	17.3	4.6	5 vol%	High filler content, use of organic solvents
PS/PPY [47]	VDP[d]	N/A	0.2	N/A	Low conductivity, use of organic solvents
PS/PPY [47]	VDP[d]	N/A	0.5	N/A	Low conductivity, use of organic solvents
PAN/PEDOT [11]	VDP[d]	9	100	N/A	Use of organic solvents
PAN/PPY [11]	VDP[d]	9	7	N/A	Use of organic solvents
PMMA/PEDOT [38]	OP[c]	10.2	0.30	7.08 wt%	High percolation threshold, low conductivity
PS/PEDOT [48]	VDP[d]	N/A	24	N/A	Use of organic solvents
PS/PPY [13]	EP[a]	17.2	$9.95\times10-4$	N/A	High filler content, low conductivity
PMMA/PEDOT (this work)	OP[c]	7.31	10.01	2.76 wt%	Low percolation threshold and one-pot water mediated

[a]Emulsion polymerization

[b]Solid-state polymerization of DBEDOT at 60–80 °C

[c]In-situ oxidative polymerization

[d]Vapor deposition polymerization

contribution of tosylate dopant was excluded. The result shows, about ~36% of the PMMA surface is covered by PEDOT when its loading level is 7.31 wt%, which is supportive to the core-shell nature of the composite as seen in morphological analysis.

Additionally, upon increasing the PEDOT content, its relative proportion at the surface also increases, confirming that PMMA microsphere is supportive for EDOT polymerization. Based on the above discussion, we consolidate that the preferential covering of PEDOT at the surface can ensure refinement in electrical conductivity by forming segregated networks.

Electrical conductivity and thermal properties of microcomposite

Neat PMMA has a very low conductivity of ~10^{-10} S/m [7, 32]. After forming the composite with PEDOT, the electrical conductivity was significantly improved (Fig. 7a and Table S1). Specifically about 10^{11} fold increase in electrical conductivity is observed for the composite compared to the PMMA matrix. The conductivity value of 10.01 S/m is reached for the composite when PEDOT loading is 7.31 wt% (Table S1). Interestingly, an abrupt rise in electrical conductivity is attained when PEDOT content is only 2.76 wt% (Fig. 7a), demonstrating the percolation behaviour of the composites. Clearly, it shows composite is fully taking the advantage of overlaid PEDOT in the PMMA matrix and thereby forming a dense conductive network. On the other hand, the conductivity of the conventional composites formed by the direct addition of EDOT, with 9.6 wt% and 15.9 wt% of PEDOT loading is only 5.4×10^{-4} S/m and 3.33×10^{-3} S/m, respectively. Also, the conductivity of the composite with 10 wt% of PEDOT loading formed via physical blending of polymer powders, is only 2.87×10^{-6} S/m. The uneven agglomeration and the distribution of PEDOT in the later composites result lower electrical conductivities as compared to our newly demonstrated method, which is more efficient in interconnecting the PEDOT surface on spherical PMMA particles as seen in morphological analysis.

A Comparison between the processing methods and electrical conductivity of one-pot water mediated composite with several CP based CPCs is given in Table 2. The main disadvantage of other composites have been mentioned based on filler content, percolation threshold, electrical conductivity and the use of harmful organic solvents. In the present composite, a high electrical conductivity with low percolation threshold ~2.76 wt% of PEDOT is attained, mainly due to the formation of segregated network. Among them, few reports provide higher electrical conductivity; however, their filler content and the processing method are undesirable. In short, our method has an advantage in terms of electrical conductivity, percolation threshold, environmental aspects, and industrial viability.

The thermogravimetric analysis (TGA) was carried out to study the thermal stability of composites. As indicated in

Table 3 Thermal Properties of PMMA and Different Composites

Sample	Ti (°C)	Tmax (°C)	Tg (°C)
PMMA	254.4	351.6	111.3
2.76 wt%	276.1	362.5	123.7
4.70 wt%	261.5	377.9	125.3
6.23 wt%	272.4	353.7	126.1
7.31 wt%	278.1	361.1	125.6
13.54 wt%	259.1	356.1	126.1

Fig. 7b, a small initial weight loss (~3 wt%) occurs till 105 °C, can be ascribed to the moisture adsorbed on the samples. For neat PEDOT, the continuous weight loss at 190–400 °C and 400–600 °C, can be considered to the degradation and carbonization of PEDOT, respectively [49]. There are two weight loss stages for PMMA [32]. The first, which observed in the range of 110–210 °C, should be assigned to the degradation of unsaturated end groups. Then, the major decomposition begins to decompose at 225 °C and degrades completely at 410 °C, which is due to the main-chain scissions of PMMA molecule.

For composites, the onset decomposition temperature was increased as compared to the neat PMMA matrix. About an increase of 21.7 and 23.7 °C (Table 3) were observed for composites with 2.76 wt% and 7.31 wt% of PEDOT contents, respectively. Moreover, the temperature at maximum decomposition rate (Tmax) of composites was also improved (Fig. 7d). It is mainly due to the formation of core-shell structure, providing an up shifted decomposition of the composites. Additionally, the weight fraction of PMMA at 410 °C is only 9.58%. Compared to the PMMA matrix, it increased to 33.7% and 50.6% for composites with 7.31 wt% and 13.54 wt% of PEDOT contents, respectively. Such improvements in thermal stability of composites verify the formation of surface enriched PEDOT on PMMA microsphere and also supportive to the segregated structure of composite. Several research reports highlight the enhanced thermal stability of composites with PMMA containing different conducting polymers.

Further, the DSC thermograms (Fig. 7c) provide the evidence for the interfacial compatibility of PEDOT and PMMA in the resultant core-shell structure of the composites. The neat PMMA shows a glass transition temperature (Tg) value of 111.3 °C [32]. Upon forming composite, an increase in Tg was observed (Table 3), assuming that physically entrapped PEDOT restricts the segmental mobility of the polymer matrix. As seen in previous discussions, the spherical PMMA surface is supportive for the decoration of PEDOT via physical interactions.

Conclusion

In summary, we have demonstrated a one-pot water mediated process for developing highly conductive microcomposites of PMMA with PEDOT as conductive network. For this, a one-pot reaction container was constantly maintained at 75 °C and N_2 atmosphere. The composite was prepared by three successive steps. The cationic polymer latex particles were generated using surfactant-free emulsion polymerization. Then, the slow addition of acoustically emulsified anionic EDOT to the cationic PMMA latex followed by the in situ oxidative polymerization generated the microcomposite. The presence of positive charge on PMMA microsphere invites the anionic EDOT emulsion towards its surface which can effectively prevent the uneven agglomeration of forthcoming in situ polymerized PEDOT. The obtained microcomposite showed promising electrical conductivity, thermal stability, and morphological characteristics. Especially, it provided an impressive enhancement in electrical conductivity by almost ~10^{11} fold compared to the PMMA matrix when PEDOT loading was only 7.31 wt%. Besides, it provided the percolation threshold at a quite low filling of 2.76 wt% of PEDOT, confirming the generation of segregated conductive networks in the matrix. The SEM and TEM images showed, the spherical PMMA particles are uniformly covered by PEDOT polymers, thanks to the electrostatic interaction and the in situ oxidative polymerization. Thermal properties have been improved by an efficient filling of PEDOT into the interstitial voids of polymer matrix. The method disclosed in this work, i.e., conductive polymer composites comprised of PMMA and PEDOT, opens up a rationally simple but an efficient route for the synthesis of polymer materials with balanced electrical and thermal properties. Also, the stable aqueous dispersion of composite could be useful in light induced applications such as photocatalysis, solar cells etc.

Supplementary Information The online version contains supplementary material available at https://doi.org/10.1007/s10965-023-03497-w.

Acknowledgements Not applicable.

Author contributions All authors have given approval to the final version of the manuscript.

Data availability All data generated or analyzed during this study are included in this published article (and its supplementary information files).

Declarations

Conflict of interest The authors declare no competing financial interest.

References

1. Chen J, Liao X, Xiao W et al (2019) Facile and green method to structure ultralow-threshold and lightweight Polystyrene/MWCNT composites with segregated conductive networks for efficient electromagnetic interference shielding. ACS Sustain Chem Eng 7:9904–9915
2. Pang H, Xu L, Yan DX, Li ZM (2014) Conductive polymer composites with segregated structures. Prog Polym Sci 39:1908–1933
3. Wang M, Tang XH, Cai JH et al (2021) Construction, mechanism and prospective of conductive polymer composites with

multiple interfaces for electromagnetic interference shielding: a review. Carbon 177:377–402
4. Bagotia N, Choudhary V, Sharma DK (2018) Superior electrical, mechanical and electromagnetic interference shielding properties of polycarbonate/ethylene-methyl acrylate-in situ reduced graphene oxide nanocomposites. J Mater Sci 53:16047–16061
5. Umoren SA, Solomon MM (2019) Protective polymeric films for industrial substrates: a critical review on past and recent applications with conducting polymers and polymer composites/nanocomposites. Prog Mater Sci 104:380–450
6. Jiang D, Murugadoss V, Wang Y et al (2019) Electromagnetic interference shielding polymers and nanocomposites - a review. Polym Rev 59:280–337
7. Jang BJ, Oh JH (2005) Fabrication of a highly transparent conductive thin film from polypyrrole / poly (methyl methacrylate) core / shell nanospheres. Adv Funct Mater 15:494–502
8. Pisuchpen T, Keaw-on N, Kitikulvarakorn K et al (2017) Electrospinning and solid state polymerization: a simple and versatile route to conducting PEDOT composite films. Eur Polym J 96:452–462
9. Hatchett DW, Josowicz M (2008) Composites of intrinsically conducting polymers as sensing nanomaterials. Chem Rev 108:746–769
10. Raman S, Ravi Sankar A (2022) Intrinsically conducting polymers in flexible and stretchable resistive strain sensors: a review. J Mater Sci 57:13152–13178
11. Laforgue A, Robitaille L (2010) Deposition of ultrathin coatings of polypyrrole and poly (3, 4-ethylenedioxythiophene) onto electrospun nanofibers using a vapor-phase polymerization method. Chem Mater 22:2474–2480
12. Kwon OS, Park SJ, Park HW et al (2012) Kinetically controlled formation of multidimensional poly(3,4-ethylenedioxythiophene) nanostructures in vapor-deposition polymerization. Chem Mater 24:4088–4092
13. Ghalib H, Abdullah I, Daik R (2013) Electrically conductive polystyrene/polypyrrole nanocomposites prepared via emulsion polymerization. Polym Plast Technol Eng 52:478–484
14. Park H, Jong S, Kim S et al (2013) Conducting polymer nanofiber mats via combination of electrospinning and oxidative polymerization. Polymer 54:4155–4160
15. Steen T, West K, Hassager O, Larsen NB (2006) Integration of conducting polymer network in non-conductive polymer substrates. Synth Met 156:1203–1207
16. Kayser LV, Lipomi DJ (2019) Stretchable conductive polymers and composites based on PEDOT and PEDOT:PSS. Adv Mater 31:1–13
17. Winther-Jensen B, West K (2004) Vapor-phase polymerization of 3,4-ethylenedioxythiophene: a route to highly conducting polymer surface layers. Macromolecules 37:4538–4543
18. Zozoulenko I, Franco-Gonzalez JF, Gueskine V et al (2021) Electronic, Optical, Morphological, Transport, and Electrochemical Properties of PEDOT: a theoretical perspective. Macromolecules 54:5915–5934
19. Kim J, Lee J, You J et al (2016) Conductive polymers for next-generation energy storage systems: recent progress and new functions. Mater Horiz 3:517–535
20. Rahimzadeh Z, Naghib SM, Zare Y, Rhee KY (2020) An overview on the synthesis and recent applications of conducting poly(3,4-ethylenedioxythiophene) (PEDOT) in industry and biomedicine. J Mater Sci 55:7575–7611
21. Leong TSH, Martin GJO, Ashokkumar M (2017) Ultrasonic encapsulation – a review. Ultrason Sonochem 35:605–614
22. Tzirakis MD, Zambail R, Tan YZ et al (2015) Surfactant-free synthesis of sub-100nm poly(styrene-co-divinylbenzene) nanoparticles by one-step ultrasonic assisted emulsification/polymerization. RSC Adv 5:103218–103228
23. Asami R, Atobe M, Fuchigami T (2005) Electropolymerization of an immiscible monomer in aqueous electrolytes using acoustic emulsification. J Am Chem Soc 127:13160–13161
24. Nakabayashi K, Yanagi H, Atobe M (2014) Preparation of W/O nanoemulsion using tandem acoustic emulsification and its novel utilization as a medium for phase-transfer catalytic reaction. RSC Adv 4:57608–57610
25. Asami R, Fuchigami T, Atobe M (2006) Development of a novel environmentally friendly electropolymerization of water-insoluble monomers in aqueous electrolytes using acoustic emulsification. Langmuir 22:10258–10263
26. Nakabayashi K, Kojima M, Inagi S et al (2013) Size-controlled synthesis of polymer nanoparticles with tandem acoustic emulsification followed by soap-free emulsion polymerization. ACS Macro Lett 2:482–484
27. Li MK, Fogler HS (1978) Acoustic emulsification. Part 1. The instability of the oil-water interface to form the initial droplets. J Fluid Mech 88:499–511
28. Li MK, Fogler HS (1978) Acoustic emulsification. Part 2. Breakup of the large primary oil droplets in a water medium. J Fluid Mech 88:513–528
29. Reddy SR, Fogler HS (1980) Emulsion stability of acoustically formed emulsions. J Phys Chem 84:1570–1575
30. Gross S, Camozzo D, Di Noto V et al (2007) PMMA: a key macromolecular component for dielectric low-κ hybrid inorganic-organic polymer films. Eur Polym J 43:673–696
31. Ali U, Karim KJBA, Buang NA (2015) A review of the Properties and Applications of Poly (Methyl Methacrylate) (PMMA). Polym Rev 55:678–705
32. Pham VH, Dang TT, Hur SH et al (2012) Highly conductive poly(methyl methacrylate) (PMMA)-reduced graphene oxide composite prepared by self-assembly of PMMA latex and graphene oxide through electrostatic interaction. ACS Appl Mater Interfaces 4:2630–2636
33. Camli ST, Buyukserin F, Balci O, Budak GG (2010) Size controlled synthesis of sub-100 nm monodisperse poly(methylmethacrylate) nanoparticles using surfactant-free emulsion polymerization. J Colloid Interface Sci 344:528–532
34. Sanchis MJ, Redondo-Foj B, Carsí M et al (2016) Controlling dielectrical properties of polymer blends through defined PEDOT nanostructures. RSC Adv 6:62024–62030
35. Master AM, Rodriguez ME, Kenney ME et al (2010) Delivery of the photosensitizer pc 4 in PEG–PCL micelles for in vitro PDT studies. J Pharm Sci 99:2386–2398
36. Zhao Q, Jamal R, Zhang L et al (2014) The structure and properties of PEDOT synthesized by template-free solution method. Nanoscale Res Lett 9:1–9
37. Bongo M, Winther-Jensen O, Himmelberger S et al (2013) PEDOT:gelatin composites mediate brain endothelial cell adhesion. J Mater Chem B 1:3860–3867
38. Saeed PA, Shilpa R, Athiyanathil S (2022) A water mediated approach for the preparation of conductive poly (3,4-ethylenedioxythiophene) decorated poly (methyl methacrylate) microcomposites. Mater Adv. https://doi.org/10.1039/d2ma00027j
39. Kim TY, Park CM, Kim JE, Suh KS (2005) Electronic, chemical and structural change induced by organic solvents in tosylate-doped poly(3,4-ethylenedioxythiophene) (PEDOT-OTs). Synth Met 149:169–174
40. Thakur VK, Vennerberg D, Madbouly SA, Kessler MR (2014) Bio-inspired green surface functionalization of PMMA for multifunctional capacitors. RSC Adv 4:6677–6684
41. Yilmaz E, Sezen H, Suzer S (2012) Probing the charge build-up and dissipation on thin PMMA Film Surfaces at the molecular level by XPS. Angew Chem 124:5584–5588

42. Nathawat R, Kumar A, Acharya NK, Vijay YK (2009) XPS and AFM surface study of PMMA irradiated by electron beam. Surf Coat Technol 203:2600–2604
43. Khan MA, Armes SP, Perruchot C et al (2000) Surface characterization of poly(3,4-ethylenedioxythiophene)-coated latexes by X-ray photoelectron spectroscopy. Langmuir 16:4171–4179
44. Mitraka E, Jafari MJ, Vagin M et al (2017) Oxygen-induced doping on reduced PEDOT. J Mater Chem A 5:4404–4412
45. Fabretto M, Zuber K, Hall C et al (2009) The role of water in the synthesis and performance of vapour phase polymerised PEDOT electrochromic devices. J Mater Chem 19:7871–7878
46. Khan MA, Armes SP (1999) Synthesis and characterization of micrometer-sized poly(3,4-ethylenedioxythiophene)-coated polystyrene latexes. Langmuir 15:3469–3475
47. Nair S, Hsiao E, Kim SH (2008) Fabrication of electrically-conducting nonwoven porous mats of polystyrene – polypyrrole core – shell nanofibers via electrospinning and vapor phase polymerization †. J Mater Chem 18:5155–5161
48. Nair S, Hsiao E, Kim SH (2009) Melt-welding and improved electrical conductivity of nonwoven porous nanofiber mats of poly(3,4-ethylenedioxythiophene) grown on electrospun polystyrene fiber template. Chem Mater 21:115–121
49. Choi JW, Han MG, Kim SY et al (2004) Poly(3,4-ethylenedioxythiophene) nanoparticles prepared in aqueous DBSA solutions. Synth Met 141:293–299